 doi:10.20944/preprints202012.0358.v1

Article

Chimeric Drug Design with a Noncharged Carrier for Mitochondrial Delivery

Consuelo Ripoll [1], Pilar Herrero-Foncubierta [1,2], Virginia Puente-Muñoz [1,a], M. Carmen Gonzalez-Garcia [1], Delia Miguel [1], Sandra Resa [2], Jose M. Paredes [1], Maria J. Ruedas-Rama [1], Emilio Garcia-Fernandez [1], Miguel Martin [3,b], Mar Roldan [3], Susana Rocha [4], Herlinde De Keersmaecker [4], Johan Hofkens [4], Juan M. Cuerva [2] and Angel Orte [1,*]

[1] Departamento de Fisicoquimica, Unidad de Excelencia de Química Aplicada a Biomedicina y Medioambiente, Facultad de Farmacia, Universidad de Granada, Campus Cartuja, 18071 Granada, Spain
[2] Departamento de Quimica Organica, Unidad de Excelencia de Química Aplicada a Biomedicina y Medioambiente, Facultad de Ciencias, Universidad de Granada, Campus Fuentenueva, 18071 Granada, Spain
[3] GENYO, Pfizer-University of Granada-Junta de Andalucía Centre for Genomics and Oncological Research. Avda. Ilustracion 114. PTS, 18016, Granada, Spain
[4] Department of Chemistry, K. U. Leuven, Celestijnenlaan 200F, B-3001, Heverlee, Belgium
[a] Present address: Interdisciplinary Institute for Neuroscience, UMR 5297, Centre National de la Recherche Scientifique, F-33076 Bordeaux, France; and Interdisciplinary Institute for Neuroscience, University of Bordeaux, F-33076 Bordeaux, France
[b] Present address: Departamento de Bioquimica y Biologia Molecular I, Facultad de Ciencias, Universidad de Granada, Campus Fuentenueva, 18071 Granada, Spain
* Correspondence: angelort@ugr.es; Tel.: +34-958243825

Abstract: Recently, it was proposed that the thiophene ring is capable of promoting mitochondrial accumulation when linked to fluorescent markers. As a noncharged group, thiophene presents several advantages from a synthetic point of view, making it easier to incorporate such a side moiety into different molecules. Herein, we confirm the general applicability of thiophene group as mitochondrial carrier for drugs and fluorescent markers, based on a new concept of nonprotonable, noncharged transporters. We implemented this concept in a medicinal chemistry application by developing an anti-tumoral, metabolic chimeric drug, based on PDHK inhibitor dichloroacetate (DCA). The promising features of the thiophene moiety as a noncharged carrier for targeting mitochondria may represent a starting point for the design of new metabolism-aimed drugs.

Keywords: Antitumor agents; Fluorescence lifetime imaging; Medicinal chemistry; Metabolic drug; Mitochondrial carrier

1. Introduction

Mitochondria are essential organelles for cellular metabolism; therefore, understanding their functioning is critical for biologists and biochemists [1, 2]. Importantly, cellular metabolism, through mitochondrial activity, plays a central role in many alterations and diseases, including cancer [3-7]. This organelle is especially important in cancer research, where it has been recently described that tumor cells can evolve in a poor niche microenvironment, or after chemo and radiotherapy stress, by metabolic reprogramming, thus displaying an unprecedented functional plasticity for survival [3-7]. Within this context, targeting of mitochondria for either visualization or sensing depends on the existence of different carriers capable of delivering the intended compound inside this organelle [8].

Mitochondria visualization using fluorescent probes has been extensively studied and yielded high- and super-resolution images of this organelle [9-11]. Moreover, fluorescent sensors that target mitochondria have been used to extract real-time chemical and physiological information [12-15], and specific drug delivery to this organelle has been developed to enhance the drug activity [16, 17].

Preprints (www.preprints.org) | NOT PEER-REVIEWED | Posted: 15 December 2020 doi:10.20944/preprints202012.0358.v1

The working mechanism of the existing carriers is based on two different properties of the mitochondrial membrane: the negative membrane potential and the selective use of the mitochondrial protein import machinery [18]. The latter implies the use of characteristic oligopeptide sequences that must be included in the probe [19]. The former depends on the incorporation of a lipophilic cation, usually a phosphonium, ammonium or pyridinium salt, in the structure of the fluorophore or drug [20-23]. In fact, one of the most employed mitochondrial delivery carrier is the triphenyl phosphonium cation (TPP), a bulky, positively-charged group [23]. Recently, it has been shown that increasing the lipophilic volume of the carrier, using methylated phenyl radicals in TPPs, further enhances mitochondrial accumulation [17, 24]. Nevertheless, this strategy is widely used but presents some drawbacks: a) the presence of cations may disrupt the membrane potential and therefore the natural functioning of the organelle, b) the intrinsic chemical characteristics of such groups make them difficult to manage/purify, and these groups are usually introduced in the last synthetic steps.

The development of a nonprotonable, noncharged and simple mitochondrial carrier could represent a new paradigm applicable not only to fluorescent probes but also to the selective transport of therapeutic drugs to mitochondria. From a synthetic point of view, the drug modification by noncharged carriers clearly represents an improvement over traditional approaches in terms of simplicity of chemical reactions, purification steps, and subsequent characterization by spectroscopic techniques. Bearing this idea in mind, we aimed to develop very simple noncharged mitochondria carriers, which were practically unknown. The working hypothesis is that species with a partial positive charge are directly generated and trapped in the interior of the mitochondrial matrix from suitable nonprotonable, noncharged species. Mitochondria are rich in reactive oxygen species (ROS) [25], and basic electron pairs can be oxidized in such environment. A neutral carrier could be transformed into a partially charged carrier by oxidation of a basic electron pair in its structure, fostering accumulation inside the organelle. In our hypothesis, a neutral carrier diffuses into the cytoplasm and enters the mitochondrial membrane, becoming trapped in the mitochondrial matrix by an oxidation reaction (Scheme 1). During the progress of our research programme, a similar mechanism to such proposal was reported by Reshetnikov and colleagues [16], based on the oxidation of ferrocene to ferrocenium cations, and by Abelha et al. [26], who employed the oxidation of the TPP moiety. Other potential candidate for oxidation-driven mitochondrial accumulation would be pyridine, a very stable aromatic substrate presenting a basic pair that can be oxidized to yield well-known pyridine oxides [27, 28]. Unfortunately, the basicity of such an electron pair is high enough for interaction with acidic lysomes, thus preventing entry in the mitochondria. Hence, we focused our attention on the electron pair of thiophene, which is essentially not basic under physiological conditions. However, thiophenes can be oxidized by oxygen-based oxidants, e.g. H_2O_2, to yield thiophene oxides and thiophene dioxides [29-33]. Indeed, thiophene carriers showed enhanced mitochondrial accumulation when linked to acridone fluorescent markers, especially designed for fluorescence lifetime imaging microscopy (FLIM) [34]. In this previous work, whereas *N*-(3-hydroxypropyl)-4-methoxy-acridone accumulated in the cell nucleus, since acridone dyes are excellent DNA binding agents [35], the addition of a terminal thiophene ring resulted in preferential delivery of the fluorescent dye to mitochondria instead of to cell nuclei [34]. Importantly, mitochondrial delivery for a noncharged, thiophene-containing acridone dye cannot be predicted by current quantitative structure-activity relation (QSAR) algorithms [36]. Therefore, confirmation of the general applicability of thiophene as mitochondrial carrier is still lacking.

Preprints (www.preprints.org) | NOT PEER-REVIEWED | Posted: 15 December 2020 doi:10.20944/preprints202012.0358.v1

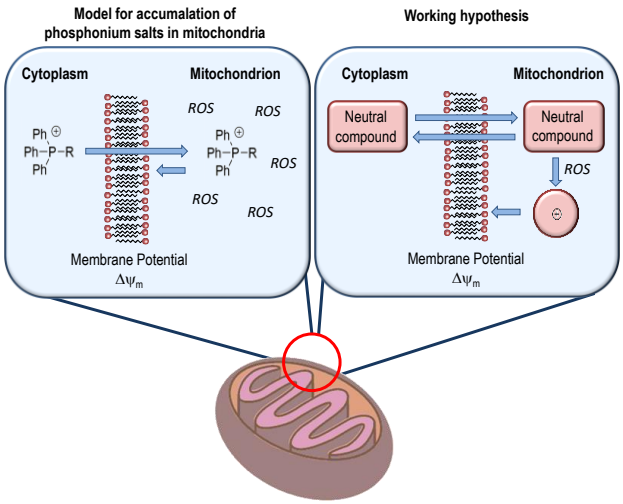

Scheme 1. Comparison of traditional mitochondrial carriers (left) and our hypothesized noncharged carriers oxidized inside mitochondria (right).

Herein, we test this new neutral mitochondrial carrier in a medicinal chemistry application, by designing a thiophene-containing chimeric drug with potential anti-cancer activity, after confirming the power of thiophene ring to achieve mitochondrial delivery. One of the key targets in the regulation of cancer metabolism is pyruvate dehydrogenase (PDH) [37], which exhibits anomalously low activity in proliferative tumors that are resistant to conventional chemotherapies. The low PDH activity is caused by hyperactive pyruvate dehydrogenase kinase (PDHK), which phosphorylates PDH. In this context, therapies aiming to reactivate PDH would have an important impact, as they may decrease the cellular metabolism to normal levels, blocking the adaptive measures of tumor cells. With this picture in mind, mitochondrial accumulation of a PDHK inhibitor may lead to enhanced effectiveness of the metabolic treatment. Dichloroacetate (DCA) is a known PDHK inhibitor, which has been tested in clinical trials, although its effectiveness has been questioned mainly because of the adverse side effects and toxicity due to the high dosages needed to achieve anti-tumoral activity [38]. Hence, we designed a very simple chimera of this PDHK inhibitor by merging DCA with a thiophene ring via an acetyl linker (**Thio-DCA**, Chart 1), and tested its effectiveness against four different breast cancer cell lines that had shown resistance to DCA treatment, MDA-MB-468, MDA-MB-231, SKBR3, and MCF7, with different metabolic features. Therefore, it is interesting to work with all these cell lines due to their different cellular and molecular features and responses to chemotherapies and treatments [39].

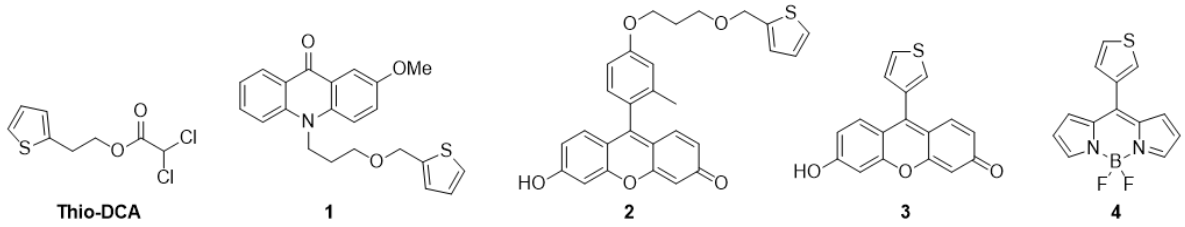

Chart 1. DCA-based drug **Thio-DCA** and thiophene-containing fluorescent dyes (acridone **1**, xanthene **2**-**3**, and BODIPY **4**) synthesized in this work.

2. Results

2.1. Synthesis of thiophene-modified fluorescent markers

In a previous work, we showed that a simple acridone-based fluorescent probe **1**, containing a thiophene side group (Chart 1), exhibited enhanced mitochondrial accumulation compared to the

Preprints (www.preprints.org) | NOT PEER-REVIEWED | Posted: 15 December 2020 doi:10.20944/preprints202012.0358.v1

thiophene-less counterpart [34]. Acridone derivatives are known to be very good DNA intercalating agents and therefore usually accumulate in the cell nucleus [35], and they are known to have very long fluorescence lifetimes, τ, which make them very suitable for FLIM imaging [41-43]. In fact, probe **1** permitted the quantitative determination of microenvironment dipolarity inside mitochondria, using the excellent sensing capabilities of the acridone moiety [34].

Encouraged by these results, we checked the performance of the thiophene group as a general mitochondrial carrier to be used in medicinal chemistry applications by its incorporation into other fluorescent compounds of different chemical nature, polarity and lipophilic characteristics (Chart 1). Apart from acridone **1**, we synthesized a xanthene derivative with the thiophene group included on a flexible chain (**2**), a xanthene derivative with the thiophene incorporated in the central ring (**3**) and a BODIPY derivative (**4**).

Both xanthene derivatives, 6-hydroxy-9-(2-methyl-4-(3-(thiophen-2-ylmethoxy) propoxy)phenyl)-3*H*-xanthen-3-one (**2**) and the thiophene-modified xanthene **3**, 6-hydroxy-9-(thiophen-3-yl)-3*H*-xanthen-3-one, were synthesized using a methodology developed by our group (Scheme 2) [44]. Thus, the addition of an organolithium derivative, obtained by bromine-lithium exchange of the corresponding aryl bromide, to the TBDMS-protected xanthene moiety afforded, after acid treatment, compounds **2** and **3**, which were isolated as orange solids. Dye **2** is a derivative of the 2-methyl-4-methoxy-phenyl xanthene, one of the so-called Tokyo Green dyes [45]. Finally, the *meso*-thiophene BODIPY, **4**, was prepared following a previously published route [40]. Further details about the synthetic protocol employed for each compound in Chart 1, as well as spectroscopic characterization (^{1}H- and ^{13}C-NMR spectral data) and mass spectrometry data, are described in the Experimental section and the Supplementary Material (SM).

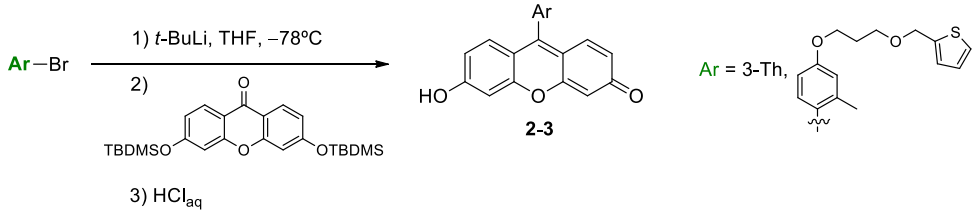

Scheme 2. Synthetic route of compounds **2**-**3**.

2.2. Thiophene as a general mitochondrial delivery agent

The synthesized thiophene-containing fluorescent markers have different structural and physical features. Whereas acridone **1** and BODIPY **4** are pH-independent and neutral fluorophores, the xanthene derivatives **2** and **3** show a prototropic equilibrium between a neutral and an anionic forms upon deprotonation of the hydroxyl group in the xanthene moiety. Using UV-visible absorption spectroscopy, we confirmed that **1** and **4** exhibited pH-independent spectra (Figure S1 in the SM), and calculated the acid–base equilibrium constant, in terms of pK_a, to be 6.28±0.06 and 6.39±0.03 for **2** and **3** (Figure S2), respectively. This mild acidic behavior may help already these dyes to be localized in mitochondria [36], but importantly, the presence of the neutral thiophene ring does not alter the acid–base properties or the charge of the dyes. Compound **2** maintained a high emission quantum yield (0.84±0.02) owed to the 2-methyl substituent in the phenyl ring, which keeps it perpendicular to the plane of the xanthene, decreasing nonradiative deactivation. The perpendicular conformation of an aromatic substituent at the *meso*- position is a well-known requirement for high fluorescence emission efficiency in xanthene [45, 46] and BODIPY [47, 48] dyes. In contrast, the thiophene ring in xanthene **3** has free rotation, decreasing the fluorescence quantum yield down to 0.14±0.01. In fact, fluorescence lifetime measurements exhibited faster deactivation, and hence a lower quantum yield, in low viscosity methanol:glycerine mixtures. At 20 ºC, the fluorescence lifetime of **3** increased from 1.7±0.1 ns in methanol (viscosity of 0.54 mPa·s) up to 2.54±0.03 ns in a methanol:glycerine mixture of 2.02 mPa·s. This dependence indicates that rotation of the thiophene ring is involved in the deactivation pathway of **3**. Further details on the viscosity dependence of the fluorescence properties of **3** can be found in Figure S3.

Preprints (www.preprints.org) | NOT PEER-REVIEWED | Posted: 15 December 2020 doi:10.20944/preprints202012.0358.v1

Once we checked that the dyes were photostable enough for imaging applications (Figure S4) and that the presence of the thiophene ring was not detrimental for the fluorescence properties of the dyes, we employed dual-color fluorescence microscopy for the simultaneous imaging of the dyes and mitochondria, which was traced in red with MitoTracker Deep Red (MT). By following the localization of the probe we could easily detect the transport efficiency of the noncharged carrier to the mitochondria. Figure 1 permitted assessment of the effective incorporation of dyes **1** and **2** into the mitochondria with great confidence. Additionally, we used dual-color FLIM microscopy to study simultaneously the localization of the dyes and their emission kinetics through the fluorescence lifetime values (see the SM and Table S1 for experimental details). Figures S5-S13 in the SM show dual-color FLIM images of dyes **1**-**4** in live cells, demonstrating a clear accumulation in the mitochondria. Nevertheless, a fraction of the dyes were also found in other cellular compartments, confirming that the accumulation is not perfectly specific, and further work may be required to achieve a higher selectivity. In fact, the Pearson's coefficient of correlation (Table S2) averaged through, at least, five different images was 0.59±0.10, 0.69±0.07, 0.58±0.12, and 0.67±0.04 for **1**, **2**, **3**, and **4**, respectively. We also obtained the mutual Manders' colocalization coefficients (MCC, Table S2) as a measure of the fraction of coincident pixels in each channel. The MCC values of colocalized dye with the MT were 0.46±0.14, 0.64±0.14, 0.58±0.15, and 0.46±0.06 for **1**, **2**, **3**, and **4**, respectively. The MCC values for the MT channel, indicating the fraction of colocalized mitochondrial pixels, were 0.64±0.10, 0.73±0.14, 0.66±0.12, and 0.36±0.12 for **1**, **2**, **3**, and **4**, respectively. These values indicate a good level of colocalization, although nonspecific, as can be visually inspected. Notably, the dye that best localized in mitochondria was **2**, in which the thiophene group is further apart the chromophore moiety. In any case, these results endorse that thiophene may be a good carrier for mitochondrial drug delivery.

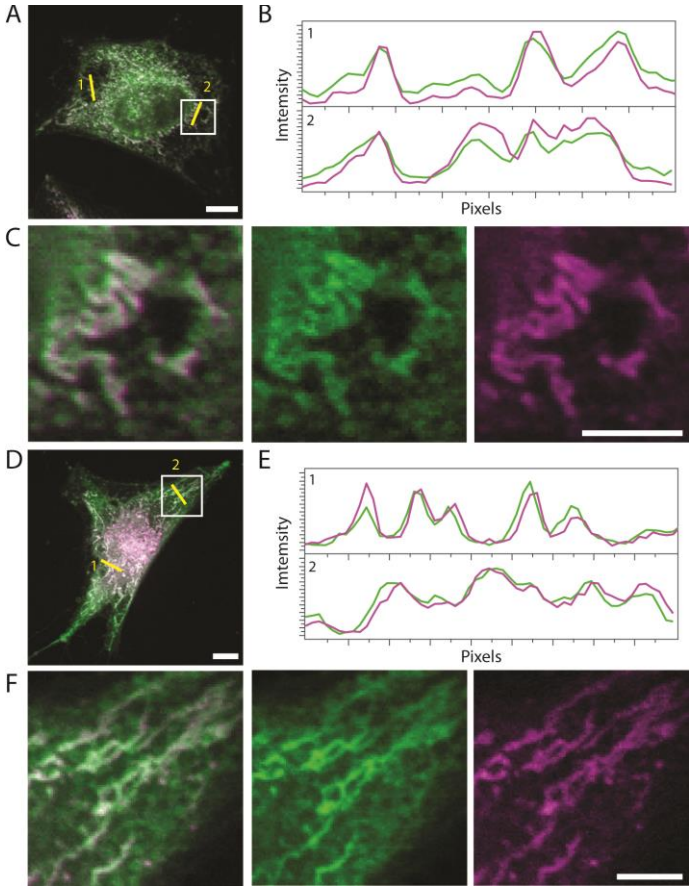

Figure 1. Dual-color confocal microscopy of **1** (A, B, and C) and **2** (D, E, and F) in formaldehyde-fixed HeLa cells. A and D) Overlaid images of the dye (green) and MT (purple). Scale bars represent 10 μm. B and E) Intensity profile traces extracted from the yellow lines in A and D. C and F) Magnified

Preprints (www.preprints.org) | NOT PEER-REVIEWED | Posted: 15 December 2020 doi:10.20944/preprints202012.0358.v1

image of the area in the white square, showing the two color channels split. Scale bars represent 5 μm.

Accumulation driven by the mitochondrial membrane potential ($\Delta\psi_m$) is usually related to positively charged lipophilic moieties, such as the TPP moiety [12]. Interestingly, dyes **1** and **4** are noncharged and neutral, and yet they accumulate in mitochondria. To evaluate whether the mitochondrial membrane potential is involved in the accumulation of the dyes in this organelle, we performed colocalization experiments of compound **1** and MT in the presence of BAM-15, a chemical known to disrupt $\Delta\psi_m$ but not affecting the plasma membrane potential and thus preventing drastic consequences on cell viability [49]. After treatment with BAM-15, the mitochondria-tracking dye, MT, was expelled out of the mitochondria and accumulated in cytoplasm vacuoles. Interestingly, a similar response was observed with the thiophene-labeled dye, **1**, which in part appeared colocalized in the vacuoles with MT but also appeared more homogeneously spread in the cytoplasm (Figure S14). These experiments revealed that the mitochondrial $\Delta\psi_m$ is directly involved in the accumulation of the thiophene-containing dyes in mitochondria. The mitochondrial targeting behavior is similar to that of MT probe, but based on a different carrying mechanism, since MT is a positively charged dye.

2.3. ***Thio-DCA***, *a PDKH inhibitor with enhanced effectiveness*

Having demonstrated the potential of the thiophene ring to enhance mithochondrial delivery of small organic molecules, we focused our attention in designing an effective mitochondrial chimeric drug, including an active agent and a specific subcellular delivery moiety [50]. The rational design of multifunctional imaging and therapeutic agents by a modular approach is an active field in current theranostics and drug discovery programmes [51-53]. As it was previously described in the introduction, cancer cells extensively rely on the glycolytic pathway to get large amounts of metabolic intermediates, which are required as building blocks to sustain their high proliferative rate. In this metabolic reprogramming process, pyruvate is reduced at the end of glycolysis to lactate, and a minor proportion is transported into the mitochondria to be transformed to acetylCoA by PDH. This metabolic pathway has been recently targeted in drug screening strategies, hypothesizing that molecules that could change the preferential metabolism of pyruvate by means of forcing its entry into mitochondrial metabolism could result specifically toxic to cancer cells. For this work, we chose DCA as a known PDHK inhibitor, capable of reactivating the PDH complex and, presumably, of switching cancer metabolism to foster mitochondria-regulated apoptosis. The main effects of DCA are a decrease in HIF-1α and Bcl-2 in neoplastic cells, followed by an increase in the expression of p-53 upregulated modulator of apoptosis, p-53 and caspases. As a consequence, a negative modulation for the transcription of GLUT receptors occurs, causing the uptake of glucose in the tumor cells to decrease [54]. Another effect of DCA on tumor cells is the increase in the generation of ROS, allowing the entry of the NADH generated in the Krebs cycle to complex I of the respiratory chain, reactivating PDH and favoring the remodeling of mitochondrial metabolism. All this cascade facilitates the opening of the mitochondrial transition pore which will allow the release to the cytoplasmic space of pro-apoptotic mediators such as cytochrome c and the apoptosis inducing factor [55].

Therefore, to enhance the effect of DCA, we synthesized the thiophene-modified DCA, **Thio-DCA**, as depicted in Scheme 3. Further details on the synthesis and characterization can be found in the experimental section and the SM.

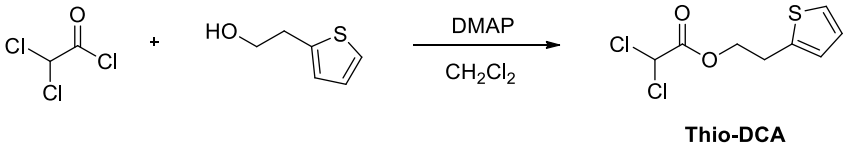

Scheme 3. Synthesis of Thio-DCA.

Preprints (www.preprints.org) | NOT PEER-REVIEWED | Posted: 15 December 2020 doi:10.20944/preprints202012.0358.v1

Regarding the cell lines employed in this work, we focused on breast cancer cells, since there exist different lines, conventionally classified according to histological type, tumor grade, lymph node status and the immune profile [39]: luminal A (cell line MCF7), luminal B (cell line ZR751), basal (cell line MDA-MB-468), claudin-low (cell line MDA-MB-231), and $HER2^+$ (cell line SKBR3). MDA-MB-468 and MDA-MB-231 are commonly referred to as triple-negative breast cancer because of its negative expression of the estrogen receptor (ER), progesterone receptor (PR) and human epidermal growth factor receptor (HER2), and present high invasiveness and poor prognostic outcome. In contrast, MCF7 and ZR751 are cell lines with a non-invasive a low proliferation character that, in turn, results in good prognostic clinical outcome. Finally, SKBR3 is a cell line that is $HER2^+$ but negative for ER and PR. According to its response to treatment, SKBR3 cells show a response to the anti-HER2 therapy Trastuzumab and a moderate response to chemotherapy. Therefore, it is interesting to work with all these cell lines due to their different cellular and molecular features and responses to chemotherapies and treatments [39]. Moreover, our recent results showed differences between these cell lines regarding intra-mitochondrial pH [14], resistance to transaminase inhibition, dependence to NAD^+ availability, and sensitivity to alterations on glutamine metabolism [56].

In a first series of experiments, the impact on cell viability by DCA-induced inhibition of PDHK was measured in the aforementioned cell lines. For this purpose, cells were seeded with or without addition of 10 mM DCA, and after 96 h incubation at 37 ºC cell viability was measured using the well-validated CellTiter Blue assay (see the Experimental section). These experiments permitted to identify that the cell lines MCF7, SKBR3, MDA-MB-231 and MDA-MB-468 were quite resistant to DCA treatment, displaying cell viability values between 75-90%. Only the cell line ZR751, with a decrease in cell viability up to 40%, resulted sensitive to DCA treatment [56]. Given we wanted to directly compare the enhanced effect of **Thio-DCA** with the corresponding native DCA, we decided not to use in further experiments the sensitive cell line ZR751, and thus only focused on the cell viability, upon incubation with **Thio-DCA**, of the DCA-resistant breast cancer lines.

Our experiments demonstrated that **Thio-DCA** presented enhanced, dosage-dependent anti-tumoral activity compared to that presented by DCA for all four studied breast cancer cell lines (Figure 2). **Thio-DCA** at 10 mM exhibited between 4.3- and 9.6-fold increase in anti-proliferation activity in the different breast cancer cell lines (Figure 2B), compared to that of DCA at the same concentration. The lowest value, a factor of 4.3-fold increase, corresponded to MDA-MB-468 cells, mainly caused by the fact that DCA 10 mM caused a mild reduction in cell viability, down to 78 ± 6 % viability. This makes that the relative effect of **Thio-DCA** compared to DCA is lower, but actually **Thio-DCA** at 10 mM in MDA-MB-468 presented the largest reduction in viability, down to 5 ± 1 %, among all the tested treatments. For the other three cell lines, 10 mM DCA did not show any significant reduction in cell viability, confirming the resistance of these cell lines to DCA treatment. Hence, the relative enhancement of the effect of 10 mM **Thio-DCA** was as large as 8.4-9.6-fold (Figure 2B). Lower concentrations of **Thio-DCA** still exhibited inhibition. For all the cell lines but MCF7, a **Thio-DCA** concentration of 5 mM resulted in a significant reduction in cell viability. The largest effect of **Thio-DCA** was found for the basal line MDA-MB-468. This cell line is characterized by a strong dependence on mitochondrial metabolism [56], and hence, our result is consistent with a larger effect of Thio-DCA due to enhanced mitochondrial delivery of the drug. In contrast, MCF7 exhibits a glycolysis-dependent metabolism [56], and in turn, the effect of **Thio-DCA** was less notable. In line, the toxic effect of **Thio-DCA** on MDA-MB-468, comes to support other experimental observations currently in progress by our team that accounts for explaining the toxicity of DCA treatments in cancer cells, which display stronger dependency on mitochondrial metabolism. According to our ongoing observations, DCA causes a metabolic collapse on mitochondrial activity due to anaplerotic limitations to respond to the DCA driven activation of tricarboxylic acid cycle.

Preprints (www.preprints.org) | NOT PEER-REVIEWED | Posted: 15 December 2020 doi:10.20944/preprints202012.0358.v1

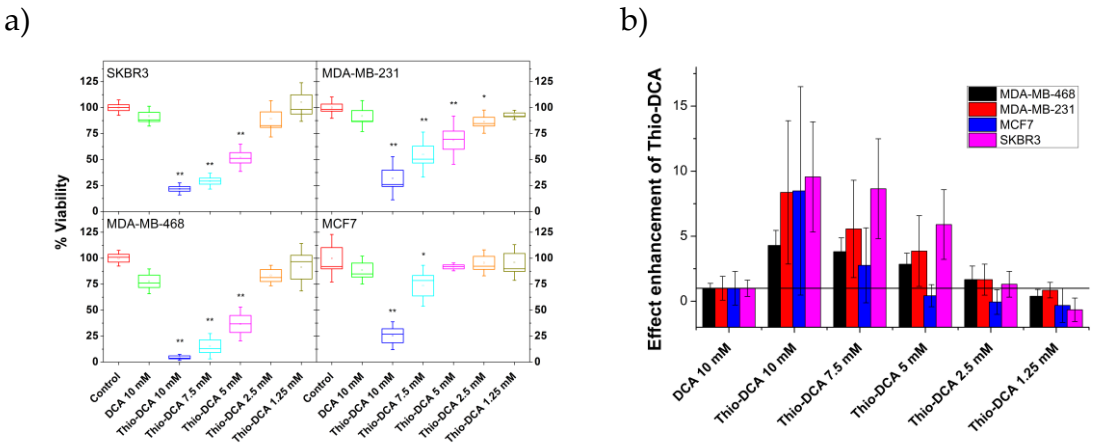

Figure 2. a) Cell viability of SKBR3, MDA-MB-231, MDA-MB-468, and MCF7 breast cancer tumor cells, treated with DCA and **Thio-DCA** at different dosages. Squares indicate mean values, the box size indicates the standard error of the mean, and whiskers represent the standard deviations. The marked populations were significantly different from the control with 99% (**) or 95% (*) confidence, as indicated by the Holm-Bonferroni and Holm-Sidak tests, and the non-parametric Kolmogorov-Smirnov and Mann-Whitney tests. b) Relative enhancement on the reduction on cell viability of **Thio-DCA** at different dosages, compared to that of DCA 10 mM.

3. Discussion

In the seeking for new, noncharged organelle-targeting carriers, we reported that neutral acridone dyes underwent mitochondrial accumulation when modified with a thiophene ring [34]. Neutral organelle carriers are vastly desired from a synthetic point of view, and regarding the effect over intraorganelle ionic strength and membrane potentials. Logically, the subsequent step was to test the general applicability of this concept, as we did herein, synthesizing thiophene-containing dyes of different families, charged (xanthenes) and noncharged (acridone and BODIPY), and confirming the enhanced mitochondrial accumulation. We have demonstrated the feasibility of the thiophene moiety as a noncharged, nonbasic carrier for targeting mitochondria. All the fluorescent derivatives synthesized herein that contain a thiophene group showed good accumulation in mitochondria, although not completely specific in part due to the additional properties that the different fluorescent moieties impart to the molecule as a whole. In previous works, fluorescent dyes containing thiophene groups were reported to be delivered to mitochondria [57-59], although the accumulation to this organelle was justified by hydrophobicity and/or the presence of positive charges in ammonium side groups. For instance, TPP-modified polythiophenes, a construct in which the polythiophene was the actual fluorophore, were shown to accumulate in mitochondria [60], although the driving force for mitochondrial delivery was assumed to be the TPP moiety. In contrast, we were able to define the different subcellular localization of dye **1** with respect to the thiophene-less acridone [34], demonstrating and confirming herein the enhancement of mitochondrial delivery by the thiophene ring. An underlying active mechanism of mitochondrial accumulation driven by the thiophene ring is supported by the fact that well-known subcellular localization QSAR algorithms [36] cannot predict such organelle targeting for dye **1**. A recent algorithm based on machine-learning, trained with sets of literature data, identified key structural motifs for subcellular localization, among lysosome, mitochondria, nucleus and plasma membrane [61]. This algorithm is included in the prediction tool admetSAR 2.0 [62]. The molecules in our work do not hold specific key motifs for mitochondria localization. In contrast, the thiophene ring was identified by the authors to be a key motif for plasma membrane localization [61]. Interestingly, admetSAR 2.0 successfully predicted all the molecules in our work would localize more likely in the mitochondria than in lysosomes, nuclei, or plasma membrane. However, the algorithm also predicted mitochondrial localization for *N*-(3-hydroxypropyl)-4-methoxy-acridone, a compound

Preprints (www.preprints.org) | NOT PEER-REVIEWED | Posted: 15 December 2020 doi:10.20944/preprints202012.0358.v1

that localizes in the cell nucleus [34]. Therefore, there is still room for improvement in machine-learning algorithms and QSAR models.

The most promising application, though, was the synthesis of **Thio-DCA** as a potential PDHK inhibitor. **Thio-DCA** has exhibited enhanced anti-tumoral activity in cell lines resistant to the thiophene-less counterpart, DCA. This enhanced toxicity suggests that the activity of the inhibitor can target the locations on mitochondrial compartments where the metabolic reactions occur. The concept of enhancing the activity of DCA with a mitochondrial-carrier was previously reported by Pathak and colleagues, who prepared a chimera of positively-charged TPP with three molecules of DCA, so-called Mito-DCA [22]. This molecule exhibited a much potent effect than DCA alone in tumoral cells, even at lower dosages than that reported by us with **Thio-DCA**. Nevertheless, Mito-DCA contains three DCA moieties per-molecule and overall a positive charge that enhanced mitochondrial depolarization [22]. In other examples, the anti-cancer power of haloacetates has been enhanced by incorporating DCA, and other derivatives, in phospholipid-nanoparticles [63]. Increasing the local concentration of the inhibitor by the nanoparticle ensured efficient delivery.

It is also informative to browse through literature of previous reports on anti-cancer drug design including thiophene cores. These drugs exhibited higher activity than previous inhibitors [64]. Likewise, thiophene-containing natural products, such as the bi-thiophenes arctinal and arctinol-b, have been shown to have antifungal and antimicrobial activity [65], as well as other cytotoxic effects on tumoral cell lines [66]. Thiophene-modified coumarins also exhibit enhanced cytotoxicity towards cancer cell lines, whereas normal fibroblast cells are less affected [67]. We hypothesize that, in some cases, the main cause of this activity may be the inhibitor accumulation in the mitochondria, which is influenced by the thiophene core and enhances the inhibition mechanism by directly targeting where the metabolic reaction occurs.

Our current research lines aim to answer whether the different subtypes of breast cancer cells display differential metabolic phenotypes [14, 56]. Gaining knowledge about metabolic key features in breast cancer and their functional, molecular and genetic interrelationships could pave the way to a novel clinical classification, finding potential therapeutic antimetabolic targets, and diagnostic approaches. The promising features of the thiophene moiety as a noncharged neutral carrier for targeting mitochondria may represent a starting point for the design of new metabolism-aimed drugs. This rationale may contribute to the field of metabolism-targeted, anti-cancer drugs [68].

4. Materials and Methods

4.1. Synthesis reactions of new compounds

General details. All reagents and solvents (CH_2Cl_2, ethyl acetate (EtOAc), hexane, CH_3CN, methanol (MeOH)) were purchased from standard chemical suppliers and used without further purification. To ensure the dryness of tetrahydrofuran (THF), it was freshly distilled over Na/benzophenone. Anhydrous solvents (dimethylformamide (DMF), CH_2Cl_2 and diethyl ether (Et_2O)) were purchased from standard suppliers. Thin-layer chromatography (TLC) was performed on aluminum-backed plates coated with silica gel 60 (230-240 mesh) with F_{254} indicator. The spots were visualized with UV light (254 nm and 360 nm) and/or stained with phosphomolybdic acid (10% ethanol solution) and subsequent heating. All chromatographic purifications were performed with silica gel 60 (230-400 mesh). NMR spectra were measured at room temperature. ^{1}H NMR spectra were recorded at 300, 400, 500 or 600 MHz. Chemical shifts are reported in ppm using the residual solvent peak as a reference ($CHCl_3$: δ = 7.26 ppm, CH_3OH: δ = 3.31 ppm, $(CH_3)_2SO$: δ = 2.50 ppm). Data are reported as follows: chemical shift, multiplicity (s: singlet, d: doublet, t: triplet, q: quartet, quint: quintuplet, m: multiplet, dd: doublet of doublets, dt: doublet of triplets, td: triplet of doublets, bs: broad singlet), coupling constant (*J* in Hz) and integration; ^{13}C NMR spectra were recorded at 75, 101, 126 or 151 MHz using broadband proton decoupling, and chemical shifts are reported in ppm using the residual solvent peaks as a reference ($CHCl_3$: δ = 77.16 ppm, CH_3OH: δ = 49.00 ppm, $(CH_3)_2SO$: δ = 39.52 ppm). Carbon multiplicities were assigned by distortionless enhancement by polarization transfer (DEPT) techniques. High-resolution mass spectra (HRMS)

Preprints (www.preprints.org) | NOT PEER-REVIEWED | Posted: 15 December 2020 doi:10.20944/preprints202012.0358.v1

were recorded by EI at 70 eV on a Micromass AutoSpec mass spectrometer (Waters) or by ESI on a Waters VG AutoSpec mass spectrometer. For the synthesis of the compounds described herein, several precursors were required to be prepared, including 2-[3-(4-bromo-3-methyl-phenoxy)propoxymethyl]thiophene (precursor **VII** in the SM) and 2,7-di-[*tert*-butyldimethylsilyloxy]-xanthone (precursor **VIII** in the SM). Compounds **1** and **4** were prepared as previously described, isolated as pure samples and showed NMR spectra identical to reported data [34, 40]. Further details on the synthesis and characterization of all the precursors and compounds **1**-**4**, including ^{1}H NMR and ^{13}C NMR spectra are compiled in the SM.

Synthesis of 6-hydroxy-9-(2-methyl-4-(3-(thiophen-2-ylmethoxy)propoxy)phenyl)-3*H*-xanthen-3-one (compound 2). To a solution of compound **VII** (279 mg, 0.82 mmol) in freshly distilled THF (4 mL) under an Ar atmosphere at –78 ºC, *t*-BuLi (1.7 M in hexane, 0.96 mL, 1.64 mmol) was added dropwise. After keeping the reaction at that temperature for 20 minutes, a solution of compound **VIII** (187 mg, 0.41 mmol) in THF (2 mL) was slowly added. Then, the mixture was stirred at –78 ºC for 15 minutes and then allowed to reach room temperature. The reaction was monitored by TLC. After consumption of compound **VIII**, HCl 10% (1 mL) was added promoting a color change from light yellow to orange. Finally, solvent was removed and residue was purified by flash chromatography (SiO_2, CH_2Cl_2/MeOH 9:1) to give compound **2** (130 mg, 66%) as an orange solid. ^{1}H NMR (400 MHz, MeOD) δ 7.36 (dd, *J* = 5.1, 1.2 Hz, 1H), 7.12 (d, *J* = 8.4 Hz, 1H), 7.08 (d, *J* = 9.7 Hz, 2H), 7.05 – 7.03 (m, 1H), 7.00 (d, *J* = 2.5 Hz, 1H), 6.99 – 6.94 (m, 2H), 6.68 – 6.64 (m, 4H), 4.72 (s, 2H), 4.17 (t, *J* = 6.2 Hz, 2H), 3.72 (t, *J* = 6.1 Hz, 2H), 2.09 (quint, *J* = 6.2 Hz, 2H), 2.02 (s, 3H). ^{13}C NMR (101 MHz, MeOD) δ 179.0 (C), 161.5 (C), 159.7 (C), 156.5 (C), 142.5 (C), 138.9 (C), 132.3 (CH), 131.5 (CH), 127.59 (CH) 127.58 (CH), 126.8 (CH), 126.0 (C), 123.4 (CH), 117.6 (CH), 115.5 (C), 113.3 (CH), 104.5 (CH), 68.3 (CH_2), 67.4 (CH_2), 66.0 (CH_2), 30.7 (CH_2), 20.0 (CH_3). HRMS (ESI): *m*/*z* $[M+H]^+$ calculated for $C_{28}H_{25}O_5S$: 473.1417 found: 473.1416.

Synthesis of 6-hydroxy-9-(thiophen-3-yl)-3*H*-xanthen-3-one (compound 3). To a solution of 3-iodothiophene (118 mg, 0.56 mmol) in freshly distilled THF (2 mL) under Ar atmosphere at –50 ºC, *t*-BuLi (1.7 M in hexane, 0.66 mL, 1.12 mmol) was added dropwise. After keeping the reaction at that temperature for 20 minutes, a solution of compound **VIII** (128 mg, 0.28 mmol) in THF (2 mL) was slowly added. Then, the mixture was stirred at –50 ºC for 15 minutes and then allowed to reach room temperature. The reaction progress was monitored by TLC. After consumption of compound **VIII**, HCl 10% (1 mL) was added promoting a color change from light yellow to orange. Finally, solvent was removed and residue was purified by flash chromatography (SiO_2, CH_2Cl_2/MeOH 8:2) to give the compound **3** (48 mg ,59%) as an orange solid. ^{1}H NMR (500 MHz, DMSO-d_6) δ 7.93 – 7.87 (m, 2H), 7.32 (dd, *J* = 4.7, 1.4 Hz, 1H), 7.22 (d, *J* = 9.3 Hz, 2H), 6.64 (bs, 4H). ^{13}C NMR (126 MHz, DMSO-d_6) δ 145.4 (C), 132.2 (C), 130.5 (CH), 129.3 (CH), 128.0 (CH), 127.7 (CH). Several carbons are not observed. HRMS (EI): *m*/*z* $[M]^+$ calculated for $C_{17}H_{10}O_3S$: 294.0351 found: 294.0339.

Synthesis of Thio-DCA. To a solution of 2-thiopheneethanol (0.26 mL, 2.34 mmol) in CH_2Cl_2 (5 mL), 4-dimethylaminopyridine (DMAP, 429 mg, 3.51 mmol) was added. After 5 minutes, dichloroacetyl chloride (0.27 mL, 2.81 mmol) was added dropwise. The mixture was stirred at room temperature and monitored by TLC until consumption of starting materials (5-10 min). Celite was then added and the solvent was removed. The crude was purified by flash chromatography (SiO_2, Hexane/EtOAc 9:1) to give the **Thio-DCA** (512 mg, 91%) as a light yellow liquid. ^{1}H NMR and ^{13}C NMR spectra are shown in the SM. ^{1}H NMR (400 MHz, $CDCl_3$) δ 7.19 (dd, *J* = 5.1, 1.2 Hz, 1H), 6.96 (dd, *J* = 5.1, 3.4 Hz, 1H), 6.90 (dd, *J* = 3.4, 1.2 Hz, 1H), 5.95 (s, 1H), 4.49 (t, *J* = 6.7 Hz, 2H), 3.25 (t, *J* = 6.7 Hz, 2H). ^{13}C NMR (75 MHz, $CDCl_3$) δ 164.5 (C), 138.7 (C), 127.2 (CH), 126.1 (CH), 124.5 (CH), 67.6 (CH_2), 64.3 (CH), 29.0 (CH_2). HRMS (ESI): *m*/*z* $[M+Na]^+$ calculated for $C_8H_8O_2Cl_2SNa$: 260.9514 found: 260.9513.

4.2. Instrumentation

Absorption spectra of the different dyes in aqueous solutions were obtained on a Lambda 650 UV–visible spectrophotometer (PerkinElemer, Whaltam, USA). The steady-state fluorescence emission and excitation spectra were collected using a Jasco FP-8300 spectrofluorometer (Jasco,

Japan). Time-resolved fluorescence decay traces were obtained on a FluoTime 200 SPT spectrofluorometer (PicoQuant GmbH, Germany). The concentration of dyes in spectroscopic measurements was between 0.5×10^{-6} and 5×10^{-6} M.

Colocalization studies using dual-color confocal microscopy were performed on a Fluoview FV1000 laser scanning microscope (Olympus, Japan). Dual-color FLIM experiments were carried out on a MicroTime 200 microscope (PicoQuant GmbH, Germany) equipped with different pulsed diode lasers as excitation sources. Further experimental settings for each instrument can be found in the SM and Table S1. The concentration of dyes in fluorescence imaging experiments was 3×10^{-7} M.

The effect of the DCA or **Thio-DCA** compounds on cell viability was studied using the CellTiter Blue™ viability assay (Promega). The cells were plated in quadruplicate in black, cell culture-treated, 96-well, optical, flat-bottom plates at a density of $8x10^{4}$ cells/well. The viability results of the different treatments were compared to those of the control (cells in the presence of deuterated DMSO) using the Mann-Whitney nonparametric test in Origin 9.0 (OriginLab Co., USA).

Further details about all the experimental methods, procedures and instrumentation can be found in the SM.

Supplementary Materials: The following are available online at www.mdpi.com/xxx/s1: details on the synthesis of precursor reagents, compounds **1**-**4** and **Thio-DCA**; ^{1}H- and ^{13}C-NMR characterization of precursor reagents, compounds **1**-**4** and **Thio-DCA**; further details on experimental procedures; Table S1: Dual-color FLIM instrumental settings for colocalization studies of each dye; Figures S1-S4: Supplementary spectroscopy figures of dyes **1**-**4**; Figures S5-S14: Additional figures from the colocalization studies of dyes **1**-**4** with MT; Table S2: Pearson's correlation coefficient (PCC) and Manders' colocalization coefficient (MCC) values for the colocalization of dyes **1**–**4** with the mitochondria tracker MT.

Author Contributions: Conceptualization, Maria J. Ruedas-Rama, Miguel Martin, Juan M. Cuerva and Angel Orte; Formal analysis, Consuelo Ripoll, Pilar Herrero-Foncubierta, Virginia Puente-Muñoz, M. Carmen Gonzalez-Garcia, Jose M. Paredes, Emilio Garcia-Fernandez and Angel Orte; Funding acquisition, Maria J. Ruedas-Rama, Juan M. Cuerva and Angel Orte; Investigation, Consuelo Ripoll, Pilar Herrero-Foncubierta, Virginia Puente-Muñoz, M. Carmen Gonzalez-Garcia, Delia Miguel, Sandra Resa, Emilio Garcia-Fernandez and Angel Orte; Methodology, Consuelo Ripoll, Delia Miguel, Jose M. Paredes, Maria J. Ruedas-Rama, Miguel Martin, Mar Roldan, Susana Rocha, Herlinde De Keersmaecker, Johan Hofkens, Juan M. Cuerva and Angel Orte; Project administration, Angel Orte; Resources, Pilar Herrero-Foncubierta, Delia Miguel, Sandra Resa, Mar Roldan, Susana Rocha, Herlinde De Keersmaecker, Johan Hofkens and Juan M. Cuerva; Supervision, Delia Miguel, Jose M. Paredes, Maria J. Ruedas-Rama, Emilio Garcia-Fernandez, Miguel Martin, Mar Roldan, Susana Rocha, Herlinde De Keersmaecker, Johan Hofkens, Juan M. Cuerva and Angel Orte; Visualization, Delia Miguel, Jose M. Paredes, Emilio Garcia-Fernandez, Susana Rocha and Herlinde De Keersmaecker; Writing – original draft, Consuelo Ripoll and Angel Orte; Writing – review & editing, Consuelo Ripoll, Pilar Herrero-Foncubierta, Virginia Puente-Muñoz, M. Carmen Gonzalez-Garcia, Delia Miguel, Sandra Resa, Jose M. Paredes, Maria J. Ruedas-Rama, Emilio Garcia-Fernandez, Miguel Martin, Susana Rocha, Johan Hofkens and Juan M. Cuerva.

Funding: This research, including APC charges, was funded by the Spanish Agencia Estatal de Investigación (Ministry of Science and Innovation) and the European Regional Development Fund [grant numbers CTQ2014-56370-R, CTQ2014-53598, and CTQ2017-85658-R]; Fundación Ramón Areces; and the initiative Solidaridad Entre Montañas. J.H. acknowledges financial support from the Flemish government through long-term structural funding Methusalem (CASAS2, Meth/15/04).

Conflicts of Interest: The authors declare no conflict of interest.

References

1. Alberts, B.; Johnson, A.; Lewis, J.; Raff, M.; Roberts, K.; Walter, P., *Molecular Biology of the Cell*. 4th Ed. ed.; Garland Science: New York, 2002. doi:
2. Scheffler, I. E., Chapter 6: Metabolic Pathways inside Mitochondria. In *Mitochondria*, 2nd Ed. ed.; John Wiley & Sons: 2007. doi:
3. Kalyanaraman, B.; Cheng, G.; Hardy, M.; Ouari, O.; Lopez, M.; Joseph, J.; Zielonka, J.; Dwinell, M. B., A review of the basics of mitochondrial bioenergetics, metabolism, and related signaling pathways in

cancer cells: Therapeutic targeting of tumor mitochondria with lipophilic cationic compounds. *Redox Biol* **2018,** 14, 316-327. doi:

4. Trotta, A. P.; Chipuk, J. E., Mitochondrial dynamics as regulators of cancer biology. *Cellular and Molecular Life Sciences* **2017,** 74, (11), 1999-2017. doi: 10.1007/s00018-016-2451-3.
5. Guerra, F.; Arbini, A. A.; Moro, L., Mitochondria and cancer chemoresistance. *Biochim. Biophys. Acta* **2017,** 1858, (8), 686-699. doi: 10.1016/j.bbabio.2017.01.012.
6. Chen, H. C.; Chan, D. C., Mitochondrial Dynamics in Regulating the Unique Phenotypes of Cancer and Stem Cells. *Cell Metab* **2017,** 26, (1), 39-48. doi:
7. Vyas, S.; Zaganjor, E.; Haigis, M. C., Mitochondria and Cancer. *Cell* **2016,** 166, (3), 555-566. doi: 10.1016/j.cell.2016.07.002.
8. D'Souza, G. G. M.; Wagle, M. A.; Saxena, V.; Shah, A., Approaches for targeting mitochondria in cancer therapy. *Biochim. Biophys. Acta* **2011,** 1807, (6), 689-696. doi: 10.1016/j.bbabio.2010.08.008.
9. Long, L.; Huang, M.; Wang, N.; Wu, Y.; Wang, K.; Gong, A.; Zhang, Z.; Sessler, J. L., A Mitochondria-Specific Fluorescent Probe for Visualizing Endogenous Hydrogen Cyanide Fluctuations in Neurons. *J. Am. Chem. Soc.* **2018,** 140, (5), 1870-1875. doi: 10.1021/jacs.7b12545.
10. Ren, M. G.; Deng, B. B.; Zhou, K.; Kong, X. Q.; Wang, J. Y.; Lin, W. Y., Single Fluorescent Probe for Dual-Imaging Viscosity and H2O2 in Mitochondria with Different Fluorescence Signals in Living Cells. *Anal. Chem.* **2017,** 89, (1), 552-555. doi:
11. Zhang, X.; Gao, F., Imaging mitochondrial reactive oxygen species with fluorescent probes: Current applications and challenges. *Free Radical Res* **2015,** 49, (4), 374-382. doi:
12. Roopa; Kumar, N.; Bhalla, V.; Kumar, M., Development and sensing applications of fluorescent motifs within the mitochondrial environment. *Chem. Commun.* **2015,** 51, (86), 15614-15628. doi: 10.1039/c5cc07098h.
13. Xu, W.; Zeng, Z.; Jiang, J.-H.; Chang, Y.-T.; Yuan, L., Discerning the Chemistry in Individual Organelles with Small-Molecule Fluorescent Probes. *Angew. Chem. Int. Ed.* **2016,** 55, (44), 13658-13699. doi: 10.1002/anie.201510721.
14. Ripoll, C.; Roldan, M.; Contreras-Montoya, R.; Diaz-Mochon, J. J.; Martin, M.; Ruedas-Rama, M. J.; Orte, A., Mitochondrial pH Nanosensors for Metabolic Profiling of Breast Cancer Cell Lines. *Int. J. Mol. Sci.* **2020,** 21, (10), 3731. doi: 10.3390/ijms21103731.
15. Sánchez, M. I.; Vida, Y.; Pérez-Inestrosa, E.; Mascareñas, J. L.; Vázquez, M. E.; Sugiura, A.; Martínez-Costas, J., MitoBlue as a tool to analyze the mitochondria-lysosome communication. *Sci. Rep.* **2020,** 10, (1), 3528. doi: 10.1038/s41598-020-60573-7.
16. Reshetnikov, V.; Özkan, H. G.; Daum, S.; Janko, C.; Alexiou, C.; Sauer, C.; Heinrich, M. R.; Mokhir, A., N-Alkylaminoferrocene-Based Prodrugs Targeting Mitochondria of Cancer Cells. *Molecules* **2020,** 25, (11), 2545. doi: 10.3390/molecules25112545.
17. Ong, H. C.; Hu, Z.; Coimbra, J. T. S.; Ramos, M. J.; Kon, O. L.; Xing, B.; Yeow, E. K. L.; Fernandes, P. A.; García, F., Enabling Mitochondrial Uptake of Lipophilic Dications Using Methylated Triphenylphosphonium Moieties. *Inorg. Chem.* **2019,** 58, (13), 8293-8299. doi: 10.1021/acs.inorgchem.8b03380.
18. Murphy, M. P., Selective targeting of bioactive compounds to mitochondria. *Trends Biotechnol.* **1997,** 15, (8), 326-330. doi: 10.1016/S0167-7799(97)01068-8.
19. Lei, E. K.; Kelley, S. O., Delivery and Release of Small-Molecule Probes in Mitochondria Using Traceless Linkers. *J. Am. Chem. Soc.* **2017,** 139, (28), 9455-9458. doi: 10.1021/jacs.7b04415.

20. Trapella, C.; Voltan, R.; Melloni, E.; Tisato, V.; Celeghini, C.; Bianco, S.; Fantinati, A.; Salvadori, S.; Guerrini, R.; Secchiero, P.; Zauli, G., Design, Synthesis, and Biological Characterization of Novel Mitochondria Targeted Dichloroacetate-Loaded Compounds with Antileukemic Activity. *J. Med. Chem.* **2016,** 59, (1), 147-156. doi: 10.1021/acs.jmedchem.5b01165.
21. Ripcke, J.; Zarse, K.; Ristow, M.; Birringer, M., Small-Molecule Targeting of the Mitochondrial Compartment with an Endogenously Cleaved Reversible Tag. *ChemBioChem* **2009,** 10, (10), 1689-1696. doi: 10.1002/cbic.200900159.
22. Pathak, R. K.; Marrache, S.; Harn, D. A.; Dhar, S., Mito-DCA: A Mitochondria Targeted Molecular Scaffold for Efficacious Delivery of Metabolic Modulator Dichloroacetate. *ACS Chem. Biol.* **2014,** 9, (5), 1178-1187. doi: 10.1021/cb400944y.
23. Zielonka, J.; Joseph, J.; Sikora, A.; Hardy, M.; Ouari, O.; Vasquez-Vivar, J.; Cheng, G.; Lopez, M.; Kalyanaraman, B., Mitochondria-Targeted Triphenylphosphonium-Based Compounds: Syntheses, Mechanisms of Action, and Therapeutic and Diagnostic Applications. *Chem. Rev.* **2017,** 117, (15), 10043-10120. doi: 10.1021/acs.chemrev.7b00042.
24. Hu, Z.; Sim, Y.; Kon, O. L.; Ng, W. H.; Ribeiro, A. J. M.; Ramos, M. J.; Fernandes, P. A.; Ganguly, R.; Xing, B.; García, F.; Yeow, E. K. L., Unique Triphenylphosphonium Derivatives for Enhanced Mitochondrial Uptake and Photodynamic Therapy. *Bioconjug. Chem.* **2017,** 28, (2), 590-599. doi: 10.1021/acs.bioconjchem.6b00682.
25. Murphy, Michael P., How mitochondria produce reactive oxygen species. *Biochem. J.* **2009,** 417, (1), 1-13. doi: 10.1042/bj20081386.
26. Abelha, T. F.; Morris, G.; Lima, S. M.; Andrade, L. H. C.; McLean, A. J.; Alexander, C.; Calvo-Castro, J.; McHugh, C. J., Development of a Neutral Diketopyrrolopyrrole Phosphine Oxide for the Selective Bioimaging of Mitochondria at the Nanomolar Level. *Chem. A Eur. J.* **2020,** 26, (14), 3173-3180. doi: 10.1002/chem.201905634.
27. Limnios, D.; Kokotos, C. G., 2,2,2-Trifluoroacetophenone as an Organocatalyst for the Oxidation of Tertiary Amines and Azines to N-Oxides. *Chem. A Eur. J.* **2014,** 20, (2), 559-563. doi:
28. Coperet, C.; Adolfsson, H.; Khuong, T. A. V.; Yudin, A. K.; Sharpless, K. B., A simple and efficient method for the preparation of pyridine N-oxides. *J. Org. Chem.* **1998,** 63, (5), 1740-1741. doi:
29. Jalilian, F.; Yadollahi, B.; Farsani, M. R.; Tangestaninejad, S.; Rudbari, H. A.; Habibi, R., New perspective to Keplerate polyoxomolybdates: Green oxidation of sulfides with hydrogen peroxide in water. *Catal. Commun.* **2015,** 66, 107-110. doi:
30. Rafiee, E.; Mirnezami, F., Keggin-structured polyoxometalate-based ionic liquid salts: Thermoregulated catalysts for rapid oxidation of sulfur-based compounds using H2O2 and extractive oxidation desulfurization of sulfur-containing model oil. *J Mol Liq* **2014,** 199, 156-161. doi:
31. Ma, B. C.; Zhao, W.; Zhang, F. M.; Zhang, Y. S.; Wu, S. Y.; Ding, Y., A new halide-free efficient reaction-controlled phase-transfer catalyst based on silicotungstate of [(C18H37)(2)(CH3)(2)N](3)[SiO4H(WO5)(3)] for olefin epoxidation, oxidation of sulfides and alcohols with hydrogen peroxide. *RSC Adv.* **2014,** 4, (61), 32054-32062. doi:
32. Tsirk, A.; Gronowitz, S.; Hornfeldt, A. B., Synthesis of Substituted Thiophene-1,1-Dioxides and Their Ring-Opening Reactions with Omega-Unsaturated Secondary-Amines - a Synthetic Route to Azatrienes. *Tetrahedron* **1995,** 51, (25), 7035-7044. doi:
33. Pouzet, P.; Erdelmeier, I.; Ginderow, D.; Mornon, J.-P.; Dansette, P.; Mansuy, D., Thiophene S-oxides: convenient preparation, first complete structural characterization and unexpected dimerization of one

of them, 2,5-diphenylthiophene-1-oxide. *J. Chem. Soc. Chem. Commun.* **1995**, (4), 473-474. doi: 10.1039/C39950000473.

34. Herrero-Foncubierta, P.; González-García, M. d. C.; Resa, S.; Paredes, J. M.; Ripoll, C.; Girón, M. D.; Salto, R.; Cuerva, J. M.; Orte, A.; Miguel, D., Simple and non-charged long-lived fluorescent intracellular organelle trackers. *Dyes and Pigments* **2020,** 183, 108649. doi: 10.1016/j.dyepig.2020.108649.
35. Thimmaiah, K.; Ugarkar, A. G.; Martis, E. F.; Shaikh, M. S.; Coutinho, E. C.; Yergeri, M. C., Drug–DNA Interaction Studies of Acridone-Based Derivatives. *Nucleosides, Nucleotides and Nucleic Acids* **2015,** 34, (5), 309-331. doi: 10.1080/15257770.2014.992531.
36. Horobin, R. W., Predicting Mitochondrial Targeting by Small Molecule Xenobiotics Within Living Cells Using QSAR Models. In *Mitochondrial Medicine: Volume II, Manipulating Mitochondrial Function*, Weissig, V.; Edeas, M., Eds. Springer New York: New York, NY, 2015; pp 13-23. doi: 10.1007/978-1-4939-2288-8_2.
37. Sullivan, L. B.; Gui, D. Y.; Heiden, M. G. V., Altered metabolite levels in cancer: implications for tumour biology and cancer therapy. *Nat. Rev. Cancer* **2016,** 16, 680. doi: 10.1038/nrc.2016.85.
38. Kankotia, S.; Stacpoole, P. W., Dichloroacetate and cancer: New home for an orphan drug? *Biochim. Biophys. Acta* **2014,** 1846, (2), 617-629. doi:
39. Holliday, D. L.; Speirs, V., Choosing the right cell line for breast cancer research. *Breast Cancer Research* **2011,** 13, (4), 215. doi: 10.1186/bcr2889.
40. Choi, S. H.; Kim, K.; Lee, J.; Do, Y.; Churchill, D. G., X-ray diffraction, DFT, and spectroscopic study of N,N′-difluoroboryl-5-(2-thienyl)dipyrrin and fluorescence studies of related dipyrromethanes, dipyrrins and BF2-dipyrrins and DFT conformational study of 5-(2-thienyl)dipyrrin. *J. Chem. Crystallogr.* **2007,** 37, (5), 315-331. doi: 10.1007/s10870-006-9126-0.
41. Smith, J. A.; West, R. M.; Allen, M., Acridones and quinacridones: Novel fluorophores for fluorescence lifetime studies. *J. Fluoresc.* **2004,** 14, (2), 151-171. doi:
42. Gonzalez-Garcia, M. C.; Peña-Ruiz, T.; Herrero-Foncubierta, P.; Miguel, D.; Giron, M. D.; Salto, R.; Cuerva, J. M.; Navarro, A.; Garcia-Fernandez, E.; Orte, A., Orthogonal cell polarity imaging by multiparametric fluorescence microscopy. *Sens. Actuator B-Chem.* **2020,** 309, 127770. doi: 10.1016/j.snb.2020.127770.
43. Ruedas-Rama, M. J.; Alvarez-Pez, J. M.; Crovetto, L.; Paredes, J. M.; Orte, A., FLIM Strategies for Intracellular Sensing. In *Advanced Photon Counting*, Kapusta, P.; Wahl, M.; Erdmann, R., Eds. Springer International Publishing: 2015; Vol. 15, pp 191-223. doi: 10.1007/4243_2014_67.
44. Martínez-Peragón, A.; Miguel, D.; Jurado, R.; Justicia, J.; Alvarez-Pez, J. M.; Cuerva, J. M.; Crovetto, L., Synthesis and Photophysics of a New Family of Fluorescent 9-alkyl Substituted Xanthenones. *Chem. A Eur. J.* **2014,** 20, 447-455. doi: 10.1002/chem.201303113.
45. Urano, Y.; Kamiya, M.; Kanda, K.; Ueno, T.; Hirose, K.; Nagano, T., Evolution of Fluorescein as a Platform for Finely Tunable Fluorescence Probes. *J. Am. Chem. Soc.* **2005,** 127, (13), 4888-4894. doi: 10.1021/ja043919h.
46. Paredes, J. M.; Crovetto, L.; Rios, R.; Orte, A.; Alvarez-Pez, J. M.; Talavera, E. M., Tuned lifetime, at the ensemble and single molecule level, of a xanthenic fluorescent dye by means of a buffer-mediated excited-state proton exchange reaction. *Phys. Chem. Chem. Phys.* **2009,** 11, (26), 5400-5407. doi: 10.1039/B820742A.
47. Yu, C.; Jiao, L.; Yin, H.; Zhou, J.; Pang, W.; Wu, Y.; Wang, Z.; Yang, G.; Hao, E., α-/β-Formylated Boron–Dipyrrin (BODIPY) Dyes: Regioselective Syntheses and Photophysical Properties. *Eur. J. Org. Chem.* **2011,** 2011, (28), 5460-5468. doi: 10.1002/ejoc.201100736.

48. Jiao, L.; Yu, C.; Wang, J.; Briggs, E. A.; Besley, N. A.; Robinson, D.; Ruedas-Rama, M. J.; Orte, A.; Crovetto, L.; Talavera, E. M.; Alvarez-Pez, J. M.; Van der Auweraer, M.; Boens, N., Unusual spectroscopic and photophysical properties of meso-tert-butylBODIPY in comparison to related alkylated BODIPY dyes. *RSC Adv.* **2015,** 5, (109), 89375-89388. doi: 10.1039/C5RA17419H.

49. Kenwood, B. M.; Weaver, J. L.; Bajwa, A.; Poon, I. K.; Byrne, F. L.; Murrow, B. A.; Calderone, J. A.; Huang, L.; Divakaruni, A. S.; Tomsig, J. L.; Okabe, K.; Lo, R. H.; Cameron Coleman, G.; Columbus, L.; Yan, Z.; Saucerman, J. J.; Smith, J. S.; Holmes, J. W.; Lynch, K. R.; Ravichandran, K. S.; Uchiyama, S.; Santos, W. L.; Rogers, G. W.; Okusa, M. D.; Bayliss, D. A.; Hoehn, K. L., Identification of a novel mitochondrial uncoupler that does not depolarize the plasma membrane. *Mol. Metab.* **2014,** 3, (2), 114-123. doi: 10.1016/j.molmet.2013.11.005.

50. Roman, G.; Popek, T.; Lazar, C.; Kiyota, T.; Kluczyk, A.; Konishi, Y., Drug Evolution Concept in Drug Design: 2. Chimera Method. *Med. Chem.* **2006,** 2, (2), 175-189. doi: 10.2174/15734060776056214.

51. Borsari, C.; Trader, D. J.; Tait, A.; Costi, M. P., Designing Chimeric Molecules for Drug Discovery by Leveraging Chemical Biology. *J. Med. Chem.* **2020,** 63, (5), 1908-1928. doi: 10.1021/acs.jmedchem.9b01456.

52. Yan, C.; Guo, Z.; Shen, Y.; Chen, Y.; Tian, H.; Zhu, W.-H., Molecularly precise self-assembly of theranostic nanoprobes within a single-molecular framework for in vivo tracking of tumor-specific chemotherapy. *Chem. Sci.* **2018,** 9, (22), 4959-4969. doi: 10.1039/C8SC01069B.

53. Yan, C.; Zhang, Y.; Guo, Z., Recent progress on molecularly near-infrared fluorescent probes for chemotherapy and phototherapy. *Coord. Chem. Rev.* **2021,** 427, 213556. doi: 10.1016/j.ccr.2020.213556.

54. Kumar, A.; Kant, S.; Singh, S. M., Novel molecular mechanisms of antitumor action of dichloroacetate against T cell lymphoma: Implication of altered glucose metabolism, pH homeostasis and cell survival regulation. *Chemico-Biological Interactions* **2012,** 199, (1), 29-37. doi: 10.1016/j.cbi.2012.06.005.

55. Ayyanathan, K.; Kesaraju, S.; Dawson-Scully, K.; Weissbach, H., Combination of Sulindac and Dichloroacetate Kills Cancer Cells via Oxidative Damage. *PLOS ONE* **2012,** 7, (7), e39949. doi: 10.1371/journal.pone.0039949.

56. Ripoll, C.; Roldan, M.; Ruedas-Rama, M. J.; Martin, M., Metabolic profiling of breast cancer cell lines. *In preparation* **2020**. doi:

57. Kawazoe, Y.; Shimogawa, H.; Sato, A.; Uesugi, M., A Mitochondrial Surface-Specific Fluorescent Probe Activated by Bioconversion. *Angew. Chem. Int. Ed.* **2011,** 50, (24), 5478-5481. doi: 10.1002/anie.201100935.

58. Jiang, N.; Fan, J.; Liu, T.; Cao, J.; Qiao, B.; Wang, J.; Gao, P.; Peng, X., A near-infrared dye based on BODIPY for tracking morphology changes in mitochondria. *Chem. Commun.* **2013,** 49, (90), 10620-10622. doi: 10.1039/C3CC46143B.

59. Griesbeck, S.; Zhang, Z.; Gutmann, M.; Lühmann, T.; Edkins, R. M.; Clermont, G.; Lazar, A. N.; Haehnel, M.; Edkins, K.; Eichhorn, A.; Blanchard-Desce, M.; Meinel, L.; Marder, T. B., Water-Soluble Triarylborane Chromophores for One- and Two-Photon Excited Fluorescence Imaging of Mitochondria in Cells. *Chem. Eur. J.* **2016,** 22, (41), 14701-14706. doi: 10.1002/chem.201602639.

60. Duca, M.; Dozza, B.; Lucarelli, E.; Santi, S.; Di Giorgio, A.; Barbarella, G., Fluorescent labeling of human mesenchymal stem cells by thiophene fluorophores conjugated to a lipophilic carrier. *Chem. Commun.* **2010,** 46, (42), 7948-7950. doi: 10.1039/C0CC01918F.

61. Yang, H.; Li, X.; Cai, Y.; Wang, Q.; Li, W.; Liu, G.; Tang, Y., In silico prediction of chemical subcellular localization via multi-classification methods. *MedChemComm* **2017,** 8, (6), 1225-1234. doi: 10.1039/C7MD00074J.

62. Yang, H.; Lou, C.; Sun, L.; Li, J.; Cai, Y.; Wang, Z.; Li, W.; Liu, G.; Tang, Y., admetSAR 2.0: web-service for prediction and optimization of chemical ADMET properties. *Bioinformatics* **2018,** 35, (6), 1067-1069. doi: 10.1093/bioinformatics/bty707.

63. Misra, S. K.; Ye, M.; Ostadhossein, F.; Pan, D., Pro-haloacetate Nanoparticles for Efficient Cancer Therapy via Pyruvate Dehydrogenase Kinase Modulation. *Sci. Rep.* **2016,** 6, (1), 28196. doi: 10.1038/srep28196.

64. Liu, K. K. C.; Zhu, J. J.; Smith, G. L.; Yin, M. J.; Bailey, S.; Chen, J. H.; Hu, Q. Y.; Huang, Q. H.; Li, C. Z.; Li, Q. J.; Marx, M. A.; Paderes, G.; Richardson, P. F.; Sach, N. W.; Walls, M.; Wells, P. A.; Zou, A. H., Highly Selective and Potent Thiophenes as PI3K Inhibitors with Oral Antitumor Activity. *Acs Med Chem Lett* **2011,** 2, (11), 809-813. doi:

65. Hanson, B. A., *Understanding Medicinal Plants. Their Chemistry and Therapeutic Action*. The Haworth Press Inc.: Binghamtom, NY, 2005. doi:

66. Zhang, P.; Liang, D.; Jin, W.; Qu, H.; Cheng, Y.; Li, X.; Ma, Z., Cytotoxic Thiophenes from the Root of *Echinops grijisii* Hance. *Z. Naturforsch.* **2009,** 64c, 193-196. doi: 10.1515/znc-2009-3-407.

67. Mohareb, R. M.; Megally Abdo, N. Y., Synthesis and Cytotoxic Evaluation of Pyran, Dihydropyridine and Thiophene Derivatives of 3-Acetylcoumarin. *Chem. Pharm. Bull.* **2015,** 63, (9), 678-687. doi: 10.1248/cpb.c15-00115.

68. Nepali, K.; Sharma, S.; Sharma, M.; Bedi, P. M. S.; Dhar, K. L., Rational approaches, design strategies, structure activity relationship and mechanistic insights for anticancer hybrids. *Eur. J. Med. Chem.* **2014,** 77, (Supplement C), 422-487. doi: 10.1016/j.ejmech.2014.03.018.